

Efficient thin-film organic solar cells based on pentacene/C60 heterojunctions

S. Yoo, B. Domercq, and B. Kippelen

Citation: *Appl. Phys. Lett.* **85**, 5427 (2004); doi: 10.1063/1.1829777

View online: <http://dx.doi.org/10.1063/1.1829777>

View Table of Contents: <http://apl.aip.org/resource/1/APPLAB/v85/i22>

Published by the [American Institute of Physics](#).

Additional information on *Appl. Phys. Lett.*

Journal Homepage: <http://apl.aip.org/>

Journal Information: http://apl.aip.org/about/about_the_journal

Top downloads: http://apl.aip.org/features/most_downloaded

Information for Authors: <http://apl.aip.org/authors>

ADVERTISEMENT



Goodfellow
metals • ceramics • polymers • composites
70,000 products
450 different materials
small quantities fast

www.goodfellowusa.com

Efficient thin-film organic solar cells based on pentacene/C₆₀ heterojunctions

S. Yoo, B. Domercq, and B. Kippelen^{a)}

Center for Organic Photonics and Electronics (COPE), School of Electrical and Computer Engineering, Georgia Institute of Technology, Atlanta, Georgia 30332

(Received 23 July 2004; accepted 6 October 2004)

We have fabricated an efficient organic photovoltaic cell based on a heterojunction of pentacene and C₆₀. Photocurrent action spectra exhibit broad light-harvesting throughout the visible spectrum with a peak external quantum efficiency (EQE) of 58±4% at short-circuit condition. Modeling studies indicate that this high EQE can be partly attributed to the large exciton diffusion length in the pentacene film as well as efficient dissociation of excitons at the pentacene/C₆₀ heterojunction.

© 2004 American Institute of Physics. [DOI: 10.1063/1.1829777]

Organic photovoltaic (PV) cells can be the versatile platforms for inexpensive solar cells and photodetectors due to the capability of being fabricated at low temperatures on various conformable substrates potentially at low cost. Over the last decade, there have been steady advances in power conversion efficiencies of devices based on small-molecule multilayer thin films^{1,2} and polymer-blend bulk heterojunctions.^{3,4} In addition to improvements in device structure and nanoscale morphology in polymer blends, choice of the right materials cannot be overemphasized in achieving high performance devices. Pentacene has been extensively studied as a *p*-type semiconductor in organic field-effect transistors,⁵ and is known to exhibit large carrier mobilities (>1 cm²/V s) within the plane parallel to the substrate.^{6–8} Due to its polycrystalline morphology, its suitability for efficient photovoltaic cells, where large charge mobility is required in a direction perpendicular to the substrate, was unclear. PV devices^{9,10} or photodetectors¹¹ fabricated with pentacene to date were mostly based on Schottky contact between metal and pentacene^{10,11} rather than organic donor/acceptor junction, and PV devices had rather low efficiencies.

In this letter, we report on photovoltaic properties of an efficient solar cell based on a junction between polycrystalline pentacene as donor and C₆₀ as acceptor. A heterojunction with electron acceptors is desired as it promotes the dissociation of excitons, and often allows broader coverage of the solar spectrum by compensating for the spectral region where absorption by pentacene is low. The device structure and the energy level diagram of the materials are shown in Fig. 1. Energy levels for these materials were borrowed from the literature.^{1,12,13} A thin layer of bathocuproine (BCP) was inserted between C₆₀ and Al as an exciton blocking layer.¹

All the organic materials were purified once by thermal gradient sublimation¹⁴ under vacuum before use. Organic layers and Al electrode were sequentially deposited in vacuum through shadow masks onto pre-cleaned indium tin oxide (ITO) substrates. The typical vacuum was 10⁻⁷ Torr during the deposition of the organic materials. ITO (15 Ω/sq.) was used as received without further treatment except for solution cleaning. Parts of ITO were etched to

define several devices with area (*A*) of approximately 0.1 cm². All the photovoltaic properties were measured in a N₂-filled glovebox without exposure of the devices to ambient air. The filtered output from a 175 W Xenon lamp (CVI, model ASB-XE-175EX) was used as a broadband light source (350–900 nm). Intensity of the incident light (*I_L*) was measured with a calibrated Si photodiode.

Electrical characteristics of a device (*A*=0.13 ±0.01 cm²) with a geometry of ITO/Pentacene (45 nm)/C₆₀ (50 nm)/BCP (10 nm)/Al are presented in Fig. 2. Under the illumination of the broadband light (*I_L*=100±2 mW/cm²), the device exhibits a short-circuit current density (*J_{SC}*) of 15±3 mA/cm², an open-circuit voltage (*V_{OC}*) of 363±3 mV, and a fill factor (*FF*) of 0.50±0.01. These values lead to a power conversion efficiency ($\eta = FF J_{SC} V_{OC} / I_L$) of 2.7±0.4%. The inset of Fig. 2 shows the forward- and reverse-bias characteristics, from which cell series resistance (*R_S**A*) and shunt resistance (*R_P**A*) are estimated to be 2.2±0.2 and 40 000±3000 Ω cm² in the dark, respectively, and to be 2.1±0.2 and 310±30 Ω cm² under illumination, respectively. The significant reduction of *R_P* under illumination can be due to the field-dependent carrier generation² and/or the photoconductive effect.⁴

In order to explain the origin of the large photocurrent and estimate the performance under the standard AM 1.5 G spectrum, external quantum efficiency (EQE), or the ratio of the number of charges generated to that of the incident photons, has been obtained as a function of wavelength (λ) [Fig. 3(a)]. It is observed that efficient light-harvesting occurs throughout the visible spectrum. The peak EQE of 58±4% is

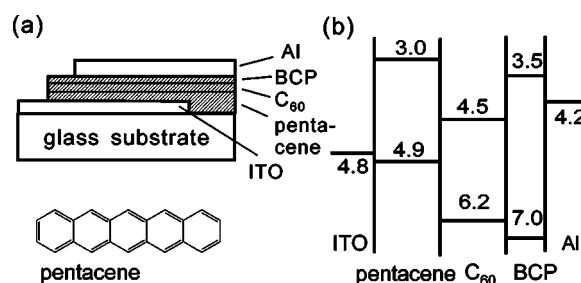


FIG. 1. (a) Schematic device structure and molecular structure of pentacene, and (b) energy diagram of a device. Energy values are approximate and given in eV with respect to the vacuum level.

^{a)} Author to whom correspondence should be addressed; electronic mail: kippelen@ece.gatech.edu

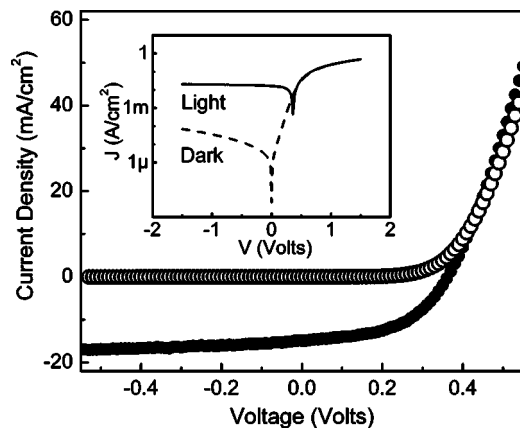


FIG. 2. Current density (J)–voltage (V) characteristics of a device with a geometry of ITO/pentacene(45 nm)/C₆₀(50 nm)/BCP(10 nm)/Al under illumination of the broadband light (100 mW/cm², 350–900 nm, closed circle) and in the dark (open circle). Inset: full-range curves in semilogarithmic scale under illumination (solid line) and in dark (dashed line).

observed at $\lambda=670$ nm at which most of the excitons are generated inside the pentacene layer considering the absorption spectrum of pentacene film¹¹ and that of C₆₀ film.¹⁵

Microscopic processes involved in the generation of photocarriers under the influence of both generation and recombination of excitons were shown to be well described by the steady-state diffusion equation^{15,16}

$$D \frac{d^2 p(z)}{dz^2} + G(z) - \frac{Dp(z)}{L^2} = 0 \quad (1)$$

in which L is the exciton diffusion length, D the diffusion coefficient, $p(z)$ the density of excitons at a location z , and $G(z)$ the density of excitons generated at z per unit time. $G(z)$ is proportional to the squared electrical field strength $|E(z)|^2$ times the absorption coefficient α .¹⁵ The solution to Eq. (1) may be expressed as

$$Dp(z) = \left(a - \frac{L}{2} \int_{z_0}^z e^{-z'/L} G(z') dz' \right) e^{z/L} + \left(b + \frac{L}{2} \int_{z_0}^z e^{+z'/L} G(z') dz' \right) e^{-z/L}, \quad (2)$$

where a and b are constants that are determined by boundary conditions at the interfaces. Then, the photocurrent J_{ph} is given by $J_{ph} = \sum_i e \eta_{CS} \eta_{CC} |D_i p'_i|$ in which i refers to either the donor or acceptor layer, p'_i is the derivative of $p_i(z)$ at the donor/acceptor interface, and η_{CS} and η_{CC} are quantum efficiencies associated with charge separation and collection, respectively.^{15,16} As described by Pettersson *et al.*, interference effect was taken into account when calculating $E(z)$ and $G(z)$.¹⁵ Equation (2) was then used to obtain $p(z)$ and J_{ph} . Boundary conditions of $p(z)=0$ at the donor/ acceptor interface and $p'(z)=0$ at the ITO/pentacene and C₆₀/BCP interfaces were imposed.¹⁶ η_{CS} and η_{CC} were assumed equal to 1. Optical constants (n, k) for each participating organic material, ITO and Al were taken from the literature.^{15–19}

The calculated field distribution at $\lambda=670$ nm indicates that $|E(z)|^2$ is enhanced in the vicinity of the junction by the presence of interference effect in a current geometry [see Fig. 3(b)]. Upon comparison of the experimental data with the calculated results for EQE as a function of the exciton

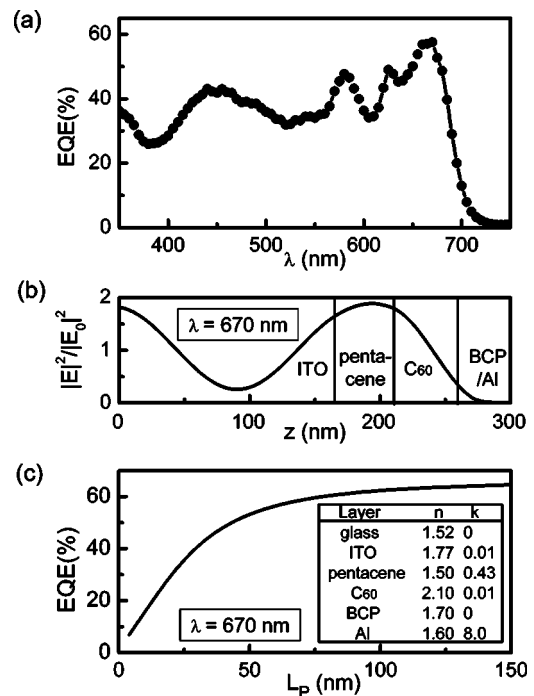


FIG. 3. (a) External quantum efficiency (EQE) vs the wavelength (λ) of the incident light. (b) Calculated distribution of the squared electric field strength, $|E|^2$, at $\lambda=670$ nm normalized by that of the incident light, $|E_0|^2$. Vertical lines indicate the location of each interface. The distance, z , is measured from the glass/ITO interface. (c) Calculated EQE as a function of pentacene diffusion length (L_p) at $\lambda=670$ nm. $L_{C60}=40$ nm was assumed. Inset: (n, k) values used for the calculation in (b) and (c).

diffusion length of pentacene (L_p) at $\lambda=670$ nm [Fig. 3(c)], L_p is estimated to be 65 ± 16 nm. The diffusion length for C₆₀ (L_{C60}) used for this calculation was 40 nm which is the value reported by Peumans, Yakimov, and Forrest¹⁶ but choice of L_{C60} had little effect on EQE at $\lambda=670$ nm because absorption by C₆₀ film is low at this wavelength. The error range in this estimation was obtained in consideration of the limited accuracies of the available optical constants for each layer. It is also advised that estimation for exciton diffusion length can yield different results depending on the model describing generation of photocurrent, boundary conditions, and other related assumptions. Exciton diffusion lengths of organic materials that were measured in various ways are summarized in Ref. 16.

Absorption profile calculated at $\lambda=670$ nm for each layer indicates 65% of the incident photons are absorbed in the pentacene layer and the others are either reflected (18%) or absorbed in the Al (12%), ITO (3%), and C₆₀ (2%) layers. The quantum efficiency of exciton-to-charge generation (QEC), or EQE divided by the absorption in the active layers,²⁰ is therefore 87%. If either of η_{CS} and η_{CC} were smaller than one, higher L_p would be needed to match the experimental result. However, QEC that is fairly close to unity suggests approximation of $\eta_{CS} = \eta_{CC} \approx 1$ may be regarded as valid and that the pentacene/C₆₀ junction serves as the site for efficient charge separation.

From the overlap integral of EQE(λ) with the distribution of photon flux under AM 1.5 G illumination, we project J_{SC} to be 8.2 ± 0.7 mA/cm² under 1 sun (100 mW/cm²).²¹ Then, η is projected to be around 1.5% under such conditions using the typical parameters at a similar level of J_{SC} . Currently, the most limiting factor is the relatively low V_{OC} .

The values reported in PV cells based on copper phthalocyanine (CuPc) and C₆₀ is around 500 mV at 1 sun level,² and those based on poly(p-phenylenevinylene) (PPV) derivatives and methanofullerene show V_{OC} over 800 mV for similar conditions.³ When the energy difference between the highest occupied molecular orbital of donor and the lowest unoccupied molecular orbital of acceptor is assumed to correlate with V_{OC},²² this difference can be attributed partly to the smaller ionization potential of pentacene compared with CuPc and PPV derivatives.

In summary, we demonstrated that high efficiency can be achieved in polycrystalline pentacene/C₆₀ heterojunctions. The spectrum of the EQE shows that efficient photoelectric conversion is possible throughout the visible range. The high EQE values in the red part of the spectrum are attributed to the large exciton diffusion length of the high-mobility polycrystalline pentacene thin film and the efficient charge separation at the junction. High photocurrent found in this type of cell demonstrates that pentacene is a promising material for high efficiency solar cells and photodetectors. When the multilayer structure is further optimized to maximize J_{SC}, and when V_{OC} is increased by the engineering of frontier orbitals, further improvement in the photovoltaic efficiency may be expected.

This material is based upon work supported in part by the STC Program of the National Science Foundation under Contract No. DMR-0120967, by the Office of Naval Research, by the National Renewable Energy Laboratory, and by a NSF CAREER program (B.K.).

¹P. Peumans and S. R. Forrest, *Appl. Phys. Lett.* **79**, 126 (2001).

²J. Xu, S. Uchida, B. P. Rand, and S. R. Forrest, *Appl. Phys. Lett.* **84**, 3013 (2004).

³S. E. Shaheen, C. J. Brabec, N. S. Sariciftci, F. Padinger, T. Fromherz, and J. C. Hummelen, *Appl. Phys. Lett.* **78**, 841 (2001).

⁴C. Waldauf, P. Schilinsky, J. Hauch, and C. J. Brabec, *Thin Solid Films* **451–452**, 503 (2004).

⁵C. D. Dimitrakopoulos and P. R. L. Malenfant, *Adv. Mater. (Weinheim, Ger.)* **14**, 99 (2002).

⁶S. F. Nelson, Y.-Y. Lin, D. J. Gundlach, and T. N. Jackson, *Appl. Phys. Lett.* **72**, 1854 (1998).

⁷T. W. Kelley, L. D. Boardman, T. D. Dunbar, D. V. Muyres, M. J. Pellerite, and T. P. Smith, *J. Phys. Chem. B* **107**, 5877 (2003).

⁸O. D. Jurchescu, J. Baas, and T. T. M. Palstra, *Appl. Phys. Lett.* **84**, 3061 (2004).

⁹R. Signerski, G. Jarosz, and J. Godlewski, *Synth. Met.* **94**, 135 (1998).

¹⁰J. Puigdollers, C. Voz, A. Orpella, I. Martin, M. Vetter, and R. Alcubilla, *Thin Solid Films* **427**, 367 (2003).

¹¹J. Lee, S. S. Kim, K. Kim, J. H. Kim, and S. Im, *Appl. Phys. Lett.* **84**, 1701 (2004).

¹²N. J. Watkins and Y. Gao, *J. Appl. Phys.* **94**, 5782 (2003).

¹³P. G. Schroeder, C. B. France, J. B. Park, and B. A. Parkinson, *J. Appl. Phys.* **91**, 3010 (2002).

¹⁴A. R. McGhie, A. F. Garito, and A. J. Heeger, *J. Cryst. Growth* **22**, 295 (1974).

¹⁵L. A. A. Pettersson, L. S. Roman, and O. Inganas, *J. Appl. Phys.* **86**, 487 (1999).

¹⁶P. Peumans, A. Yakimov, and S. R. Forrest, *J. Appl. Phys.* **93**, 3693 (2003).

¹⁷R. A. Synowicki, *Thin Solid Films* **313–314**, 394 (1998).

¹⁸S. P. Park, S. S. Kim, J. H. Kim, C. N. Whang, and S. Im, *Appl. Phys. Lett.* **80**, 2872 (2002).

¹⁹M. J. Weber, *Handbook of Optical Materials* (CRC, Boca Raton, FL, 2003), pp. 314–316.

²⁰L. A. A. Pettersson, L. S. Roman, and O. Inganas, *J. Appl. Phys.* **89**, 5564 (2001).

²¹This calculation method requires the linear response of the photocurrent with respect to the light intensity. We confirmed that this cell shows such linearity at least up to J_{SC}=15 mA/cm².

²²C. J. Brabec, A. Cravino, D. Meissner, N. S. Sariciftci, T. Fromherz, M. T. Rispens, L. Sanchez, and J. C. Hummelen, *Adv. Funct. Mater.* **11**, 374 (2001).